Metastatic Ocular Melanoma to the Liver Exhibits Infiltrative and Nodular Growth Patterns

Hans E. Grossniklaus, MD[a,b], Qing Zhang, MD, PhD[a], Shuo You,MD, PhD[b], Conni McCarthy, DrSc, MSc, BSc[c], Steffen Heegaard, MD, DMSc[d,e], Sarah E. Coupland, MBBS, PhD[c]

[a]Department of Ophthalmology, Emory University School of Medicine, Atlanta, GA
[b]Winship Cancer Institute, Emory University, Atlanta, GA
[c]Molecular and Clinical Cancer Medicine, Royal Liverpool and Broadgreen University Hospital NHS Trust, University of Liverpool, Liverpool, UK
Departments of [d]Pathology and [e]Ophthalmology, University of Copenhagen, Copenhagen, Denmark

Supported in part by NIH R01CA176001, NIH P30EY06360, and an unrestricted Departmental Grant from Research to Prevent Blindness

Correspondence to: Hans E. Grossniklaus MD, L.F. Montgomery Ophthalmic Pathology Laboratory, BT428 Emory Eye Center, 1365 Clifton Road, Atlanta, GA 30322 email: ophtheg@emory.edu

Summary

We examined liver specimens from 24 patients with uveal melanoma (UM), including 15 patients who had succumbed to their disseminated disease. We found two distinct growth patterns of UM metastasis: infiltrative (n=12) and nodular (n=3). In the *infiltrative* pattern, individual UM cells with a CD133+ cancer stem cell-like phenotype were present and formed aggregates of Stage I <50µm diameter micrometastases in the sinusoidal spaces. These micrometastases appeared to expand, destroy adjacent hepatocytes and form Stage II 51-500µm diameter and then Stage III >500µm diameter metastases, which were encapsulated by collagenized fibrous septae. In the *nodular* growth pattern, CD133+ melanoma cells aggregated adjacent to portal venules, and subsequently appeared to grow and efface the adjacent hepatocytes to form Stage II 51-500µm diameter nodules that surrounded the portal venule. These avascular nodules appeared to further expand to form Stage III >500µm diameter nodules that exhibited vascularization with minimal fibrosis. The tumor stem cell-like phenotype seen in individual UM cells was lost as the tumors progressed. There were CD56+ natural killer (NK) cells in sinusoidal spaces and CD3+ lymphocytes in periportal areas. The nodular growth pattern showed UM cells expressing MMP9 and VEGF. UM cells in both above-described growth patterns exhibited variable BAP1 expression. We propose that changes in the liver microenvironment are related to metastatic UM growth. These include immune regulation within the sinusoidal space for the infiltrative pattern and changes in the VEGF:PEDF ratio for the nodular pattern.

1.0 Introduction

Uveal melanoma (UM) is the most common primary intraocular malignancy in adults with an annual incidence of 6-7 cases/1,000,000 in the Caucasian population.[1] Approximately 40% of UM metastasize to the liver within 10 years of diagnosis of the primary intraocular tumor[2], and when UM metastasizes, the liver is typically the initial site of metastasis in 95% of cases.[3] The life expectancy of patients with metastatic UM is only 4 to 6 months[1], and at present there are no highly effective treatments for these metastases.[4]

The Zimmerman hypothesis, which was formulated in the late 1970s, proposed that enucleation of the eye for UM potentiated hematogenous spread of the tumor and a 2-year post-enucleated risk of death.[5] This theory was subsequently disproven, particularly when investigators calculated primary and metastastic UM doubling times. Their extrapolation demonstrated that small, clinically undetectable UM micrometastases were present in the liver, even at the time of diagnosis of the primary intraocular tumor in patients who ultimately succumbed from hepatic metastasis.[6] Our laboratory corroborated those results when we found small hepatic UM micrometastases in liver specimens obtained post-mortem from patients who died from metastastic UM.[8]

In our prior study[8], we found three Stages of metastases: Stage I: <50µm diameter micrometastases within the sinusoidal space; Stage II: 51-500µm diameter metastases that formed expanded collections of cells within the sinusoidal space; and Stage III: >500µm diameter collections of cells that formed two patterns. We characterized the two Stage III patterns as the ‘lobular’ and ‘portal’ patterns.[8] The lobular pattern appeared to be an expansion of Stage I to III intra-sinusoidal growth, which infiltrated the portal lobule and was surrounded by fibrous septae. In contrast, the portal pattern appeared to efface, rather than infiltrate, the surrounding liver; we hypothesized that the portal pattern arose in the perivascular area of the portal triad.[8]

In this study, we examined liver specimens from an additional 24 cases, including 15 UM patients who had died from metastatic disease. We examined for the growth stages and growth patterns as previously described[8] and explored mechanisms that

may account for these growth patterns. Based on our findings, we propose the term “infiltrative” for the lobular pattern and nodular” for the portal pattern.

2.0 Materials and Methods

This study was approved by the Emory University School of Medicine Institutional Review Board, Atlanta, Georgia. Sections of livers obtained post-mortem from patients who had UM were obtained from the Department of Molecular and Clinical Cancer Medicine, Royal Liverpool and Broadgreen University, Liverpool, UK (CM, SEC) and the Department of Ophthalmology, University of Copenhagen, Copenhagen, Denmark (SH). The patients’ samples had been pseudoanonymized for data other than age, sex, and cause of death. For each case, sections of the livers including an area of suspected metastasis found during autopsy were obtained. The sections were fixed in 10% neutral buffered formalin, routinely processed, and 4-µm sections were obtained by a microtome and placed on slides. The sections measured from 2.0cm X0.9 cm to 3.4cm X2.6cm. Sections from each case were stained with hematoxylin and eosin (H&E) and Masson trichrome (MT).

Immunohistochemical (IHC) staining using the avidin-biotin complex technique (Dako, Carpinteria, CA) was used to stain other sections from each case for HMB45 (1:50), BAP1 (C-4, Santa Cruz, Insight Biotechnology Ltd,. Middlesex, UK, 1µg/ml^{-1}), CD3 (Leica Microsystems, Bannockburn, IL, prediluted), CD20 (Leica Microsystems, prediluted) and CD31 (Dako,1:180). A red chromogen (Vector Red) was used for HMB45 and BAP1, and a brown chromogen (DAB) was used for CD3, CD20 and CD31. For immunofluorescence (IF) staining, sections of the livers were blocked in normal goat serum (5%) in PBS, followed by incubation with primary antibody. After washing, sections were incubated with appropriate fluorescent-conjugated secondary antibody, counterstained with 4',6-diamidino-2-phenylindole (DAPI, Vector Laboratories), and mounted (Vector Laboratories). IF staining for each case was performed for CD56 (R&D Systems, Minneapolis, MN), CD 133 (Biorbyt, San Francisco, CA), HMB45 (ABCAM, Cambridge, MA), MMP9 (Cell Signaling Technology, Boston, MA), VEGF (AMCAM) and a dual label HMB45/CD133. IF was examined by confocal microscopy (Nikon CI R1, Tokyo, Japan). The H&E, MT and IHC stained slides were examined by

light microscopy to determine the presence and distribution of Stage I, Stage I and Stage III metastases as previously described.[8] The number of these three stages of metastases was determined for each section in triplicate (40X, Olympus BHTU, Tokyo, Japan) and the averages of these numbers was used as the count of Stage I, Stage II and Stage III metastases per section which was normalized to number of metastases per cm^2. The presence or absence of nuclear or cytoplasmic IHC and IF staining for each antibody or dual-labelled section was recorded. For CD31, the presence and location of endothelial cells staining was recorded.

3.0 Results

We examined autopsy liver sections from 24 UM patients, including 13 men and 11 women. The average age at the time of death was 55 years, with a range from 23 to 75 years. Of the 24 cases, 9 patients died of causes other than metastatic UM. Liver sections of those 9 patients did not contain metastatic UM. Examination of liver sections of all of the remaining 15 patients who died from metastatic UM showed metastastic disease at various stages.[8] The predominant growth pattern, including all three stages in 12 patients, was infiltrative and the predominant growth pattern in the remaining 3 patients was nodular. In the livers showing an infiltrative UM growth pattern the number of metastases in order of decreasing frequency was Stage I >> Stage II > Stage III; whereas there were much fewer Stage I, II and III UM metastases in livers that exhibited the nodular pattern as shown in **Figure 1**.

IHC stains for BAP1 were positive in 6 of 12 infiltrative pattern and 1 of 3 nodular pattern metastases. The BAP1 staining was positive both in the nucleus and cytoplasm. Many that exhibited positive BAP1 staining also contained aggregates of tumor cells that were negative for BAP1. IF stains were also positive for CD56 in NK cells in the sinusoidal space and IHC stains for CD3 for T cells in the periportal area (**Figure 2**). The histopathologic, IHC and IF results in both growth patterns are summarized in **Table 1**.

The *infiltrative* growth pattern exhibited melanoma growth within the sinusoidal space. All 12 cases of predominantly infiltrative growth pattern contained individual melanoma cells within the sinusoidal space (**Figure 3**), which demonstrated positive

immunostaining for HMB45. Dual labeling showed that many of the individual HMB45 melanoma cells within the sinusoidal space also labeled for CD133. All cases exhibited Stage I HMB45 positive islands of micrometastatic UM that measured up to 50µm in diameter (**Figure 4**). These cases also contained Stage II metastases (**Figure 5**), which appeared as expansions of Stage I UM; the micrometastases had formed 51-500µm diameter aggregates, with disappearance of the adjacent hepatocytes. These UM metastases expressed MMP9 but not VEGF. There were occasional Stage III metastases (**Figure 6**), which measured greater than 500µm in diameter, and were composed of larger expansions of melanoma cells that were now surrounded by fibrous septae demonstrated with a trichrome stain. The Stage III metastases failed to express MMP9 or VEGF. All three stages of the infiltrative growth pattern did not contain CD31+ vascular channels within the tumor, although there were CD31 vascular channels present in the surrounding fibrous septae. Rare individual HMB45/CD133 melanoma cells appeared to decrease in number as the stages progressed.

The *nodular* growth pattern predominantly contained nodules of tumor that effaced, rather than infiltrated, the adjacent hepatocytes. In this growth pattern, individual melanoma cells, which expressed an HMB45/CD133 tumor stem cell-like phenotype were present in portal venules within the portal triad as well as the periportal area (**Figure 7**). There were CD3+ lymphocytes present in this area. Stage II metastases (**Figure 8**) were composed of nodules of tumor that appeared as expansions of tumor within the fibrovascular septae of the portal triad. Tumor nodules were adjacent to and/or surrounded the portal venule and effaced the surrounding hepatocytes. These nodules expressed MMP9 and VEGF. Stage III nodular growth pattern tumor (**Figure 9**) contained CD31+ vascular channels, exhibited MMP9 and VEGF expression and the vascular channels were within the nodule and at its advancing edge.

4.0 Discussion

Whilst significant progress has been made in our understanding of primary UM over the last decade, there are only a few studies on human metastatic UM to the liver, due to the relative difficulty in accessing this material, since many UM patients do not

undergo laparoscopic staging or abdominal surgery. Some recent studies (including our own), however, have undertaken morphological, immunohistochemical and genetic analyses of metastatic UM.[8-14]

Our laboratory has previously described the progression of metastatic UM to the liver in 10 patients who succumbed to the tumor to exhibit three histologic stages and two growth patterns, lobular and portal.[8] In the current study of an additional 24 cases including 15 patients who died from metastatic UM to the liver, we expanded our findings. We chose to use the term *infiltrative* rather than lobular and *nodular* rather than portal growth patterns, as we feel that the new terms better describe the pathologic findings as well as correspond to the biologic processes.

Current evidence suggests that primary UM undergoes a series of mutational events that allow it to develop and metastasize. Somatic *GNAQ* or *GNA11* mutations initiate the melanocytic neoplastic proliferation leading to nevi and UM in 85% of cases.[12] Metastasis predictors in UM include clinical factors (tumor size, ciliary body involvement, extraocular spread); histological features (epithelioid cytomorphology, mitotic count, closed laminin loops); and genetic findings (chromosome 3 loss, chromosome 8q gain, *BAP1* deletion, class 2 gene expression profile, and lack of *SF3B1* and *EIF1AX* mutations).[15-19] It is not known in which sequence later genetic alterations occur, which aberrations contribute to the malignant phenotype, which ones enable metastasis, and whether any explain why metastases almost always involve the liver. That being said, it is clear that many metastatic UM cases demonstrate chromosome 3 loss, polysomy 8q, and have BAP1 inactivating mutations. Indeed, BAP1 immunostaining of metastatic UM showed that BAP1 expression was absent in 77% cases in one study.[9] Our finding in this study of variable BAP1 expression in hepatic metastases of UM in both infiltrative and nodular tumors, including variable expression within a given liver section, supports the concept that although BAP1 mutations are important for promoting UM metastasis, the BAP1 mutation may or may not be lost in the metastases in the liver.

During the metastatic process in cancer, it is hypothesized that only a small percentage of cells (i.e. single clones) is released from a primary tumor, and ultimately one clone successfully forms distant colonies.[20] These clones could be composed of

mature differentiated cells, or of immature stem cell-like neoplastic cells. The advantage of the latter is that they are less immunogenic, and thereby can avoid the immune surveillance system present in the blood and many organs, on dissemination. There is some evidence that metastatic UM cells exhibit cancer stem cell-like phenotypes.[21-23] Our findings of dual-labeled CD45/CD133 individual UM cells in the sinusoidal space, portal venule and periportal area provides further evidence of a cancer stem cell-like phenotype of UM, as a precursor to Stages I-III metastases. Many metastatic UM cells that survive in the liver appear to be 'dormant' and not proliferating.[20] As we currently understand the process of metastatic UM to the liver, primary UM expressing high levels of c-Met and/or CXCR4 aggregate in the liver, which contains the c-Met ligand, HGF/SF and the CXCR4 ligand, SDF.[24,25] Individual UM cells that have a CD133+ tumor stem cell-like phenotype appear to give rise to the infiltrative or nodular growth patterns, depending on whether the tumor is in the sinusoidal space or periportal area (**Figure 10**). There may be stochastic properties related to the branching pattern of the sinusoidal space that are related to the ability of individual metastatic UM cells to aggregate and form micrometastases in the infiltrative growth pattern.[8] The sinusoidal space contains resident NK cells, as demonstrated in this study, and boosting of these NK cells eliminates micrometastatic UM in the liver in an animal model.[26] Other immune related cells in the sinusoidal microenvironment may change during tumor progression, including an M1 to M2 macrophage phenotypic shift.[27]

Our previous work has indicated that 0-50μm micrometastases receive their nutrition form blood in the sinusoidal space and larger infiltrative pattern metastases develop "pseudosinusoidal" spaces from stellate cells.[8] This appears to obviate the need for angiogenesis in the infiltrative growth pattern. In this study, we observed tumor MMP9 expression in Stage II infiltrative tumors, which we hypothesize is due to tumor hypoxia. This MMP production allows the melanoma to dissect through tissue planes and stellate cell proliferation leads the creation of pseudosinusoidal spaces[8], thus allowing tumor nutrition and oxygenation and obviating angiogenesis. Interestingly, we did not observe MMP9 expression in Stage III infiltrative melanoma. Alternatively, tumor cells may arise in the perivascular tissue of the portal triad[8], and in this study we demonstrate a predominance of CD3+ T cells in that area. Although this periportal

space is not exposed to the NK cells in the sinusoidal space, there is experimental evidence that proteins, such as PEDF secreted by hepatocytes, counteracts VEGF produced by melanoma cells and vascular endothelium, thus limiting tumor angiogenesis.[28] Hypoxia results in increased HIF1α and downstream MMP and VEGF production.[29] PEDF is degraded by MMP2 and MMP9[30]; our study shows MMP9 and VEGF expression in Stages II and III nodular growth pattern melanoma, and supports the concept of MMP9 degradation of PEDF and a local change in the microenvironment favoring an increased VEGF:PEDF ratio with resultant tumor angiogenesis. Our hypothesis of metastatic UM progression relative to the hepatic microenvironment is shown in **Figure 11**.

Interestingly, other studies have shown growth patterns of metastatic colon cancer to the liver, which are similar to our study of metastatic UM.[31,32] Those studies have shown a replacement pattern, which is very similar to the infiltrative pattern, the pushing pattern, which is very similar to the nodular pattern, and the desmoplastic pattern, which is similar to the Stage III infiltrative pattern. Those studies show that the replacement (infiltrative) pattern arises within the sinusoidal space and the pushing (nodular) pattern arises in the space of Disse. Our laboratory has found that mouse models of metastatic UM to the liver recapitulate the infiltrative and nodular growth patterns (unpublished data). These models support the proposed mechanisms of metastatic UM growth in the liver, including NK control of the infiltrative pattern and PEDF control in the nodular pattern.[28,33]

Recognition of the varying growth patterns of metastatic UM to the liver has clinical implications. For instance, the infiltrative and nodular growth patterns may be radiographically identified, with the nodular pattern being more amenable to chemoembolization and radioemboloization, as it is vascularized compared with the infiltrative pattern.[34,35] MRI contrast agents are currently being developed that may enable detection of early stage infiltrative versus nodular growth patterns.[36] Additionally, the choice of chemotherapeutic agents under development may be influenced by the infiltrative versus nodular growth patterns.[37]

In conclusion, we have shown that uveal melanoma metastasizes to the liver first in the form of single cells, followed by progressive stages. The single cell metastases

have cancer stem cell-like characteristics. These metastases result in the infiltrative and nodular growth patterns. We hypothesize that the following sequence of events is related to the formation of these two patterns. In the infiltrative pattern, melanoma invades the sinusoidal space, replaces the hepatic lobule, is essentially avascular, and does not express VEGF. Hypoxia results in melanoma MMP production, the creation of pseudosinusoidal spaces, and tumor oxygenation. In the nodular growth pattern, melanoma arises in the periportal area, co-opts the portal venule, and eventually grows, becomes hypoxic, expresses MMP9 and VEGF, undergoes angiogenesis, and effaces the adjacent hepatocytes. We propose that infiltrative growth is controlled in part by changes in the immune microenvironment in the sinusoidal space and nodular growth is controlled in part by the microenvironment VEGF:PEDF ratio in the periportal area.

Acknowledgements: We wish to thank Mica Duran for providing Figure 10 and John Lattier PhD for providing Figure 11.

References

(1) Cerbone L, Van GR, Van den Oord J et al. Clinical presentation, pathological features and natural course of metastatic uveal melanoma, an orphan and commonly fatal disease. *Oncology* 2014;86:185-189.
(2) Singh A, Shields C, Shields J. Prognostic factors in uveal melanoma. Mel Res 11, 255-263. 2001.
(3) Stang A, Jockel KH. Trends in the incidence of ocular melanoma in the United States, 1974-1998. *Cancer Causes Control* 2004;15:95-96.
(4) Augsburger JJ, Correa ZM, Shaikh AH. Effectiveness of treatments for metastatic uveal melanoma. *Am J Ophthalmol* 2009;148:119-127.
(5) Singh AD, Rennie IG, Kivela T, Seregard S, Grossniklaus H. The Zimmerman-McLean-Foster hypothesis: 25 years later. *Br J Ophthalmol* 2004;88:962-967.
(6) Eskelin S, Pyrhonen S, Sommanen P, Hahka-Kemppinen M, Kivela T. Tumor doubling times in metastatic malignant melanoma of the uvea: tumor progression before and after treatment. *Ophthalmology* 107, 1443-1449. 2000.
(7) Singh AD. Uveal melanoma: implications of tumor doubling time [letter]. *Ophthalmlology* 108, 829-830. 2001.
(8) Grossniklaus HE. Progression of ocular melanoma metastasis to the liver: The 2012 Zimmerman Lecture. *JAMA Ophthalmol* 2013;1-8.
(9) Kalirai H, Dodson A, Faqir S, Damato BE, Coupland SE. Lack of BAP1 protein expression in uveal melanoma is associated with increased metastatic risk and has utility in routine prognostic testing. *Br J Cancer* 2014;111:1373-1380.
(10) McCarthy C, Kalirai H, Lake SL, et al. *Pigment Cell Melanoma Res* 2016; 29:60-7
(11) Meir T, Dror R, Yu X, et al. (2007) Molecular characteristics of liver metastases from uveal melanoma. *Inv Ophthalmol Vis Sci* 2007; 48:4890-4896
(12) Griewank KG,, van de Nes J, Schilling B, et al. Genetic and clinico-pathologic analysis of metastatic uveal melanoma. *Mod Pathol* 2014; *27:*175-183
(13) Luscan A, Just PA, Briand A, Burin des Roziers C, et al. Uveal melanoma hepatic metastases mutation spectrum analysis using targeted next-generation sequencing of 400 cancer genes. *Br J Ophthalmol* 2015; 99:437–439
(14) Trolet J, Hupe P, Huon I, et al. Genomic profiling and identification of high-risk uveal melanoma by array CGH analysis of primary tumors and liver metastases. *Inv Ophthalmol Vis Sci*, 2009; 50*:*2572-2580
(15) Harbour JW, Onken MD, Roberson ED, et al. Frequent mutation of BAP1 in metastasizing uveal melanomas. *Science* 2010;330:1410-1413.
(16) Harbour JW, Roberson ED, Anbunathan H, et al. Recurrent mutations at codon 625 of the splicing factor SF3B1 in uveal melanoma. *Nature Genetics.* 2013;45:133-135.
(17) Martin M, Masshofer L, Temming P, et al. Exome sequencing identifies recurrent somatic mutations in EIF1AX and SF3B1 in uveal melanoma with disomy 3. *Nature Genetics.* 2013;45:933-936.
(18) Furney SJ, Pedersen M, Gentien D, et al. SF3B1 mutations are associated with alternative splicing in uveal melanoma. *Cancer Discovery.* 2013;3:1122-1129.
(19) Damato B, Eleuteri A, Taktak AF, Coupland SE. Estimating prognosis for survival after treatment of choroidal melanoma. *Prog Retin Eye Res.* 2011;30:285-95.

(20) Luzzi KJ, MacDonald IC, Schmidt EE et al. Multistep nature of metastatic inefficiency: dormancy of solitary cells after successful extravasation and limited survival of early micrometastases. *Am J Pathol* 1998;153:865-873.
(21) Chang SH, Worley LA, Onken MD, Harbour JW. Prognostic biomarkers in uveal melanoma: evidence for a stem cell-like phenotype associated with metastasis. *Melanoma Res* 2008;18:191-200.
(22) Kalirai H, Damato BE, Coupland SE. Uveal melanoma cell lines contain stem-like cells that self-renew, produce differentiated progeny, and survive chemotherapy. *Invest Ophthalmol Vis Sci* 2011;52:8458-8466.
(23). Thill M, Berna MJ, Brierson R, et al. Expression of CD133 and other putative stem cell markers in uveal melanoma. *Melanoma Res* 2011;25:405-416.
(24) Bakalian S, Marshall JC, Logan P et al. Molecular pathways mediating liver metastasis in patients with uveal melanoma. *Clin Cancer Res* 2008;14:951-956.
(25) Hendrix MJ, Seftor EA, Seftor RE, et al. Regulation of uveal melanoma interconverted phenotype by hepatocyte growth factor/scatter factor (HGF/SF). *Am J Pathol* 1998;152:855-863
(26) Yang H, Dithmar S, Grossniklaus HE. Interferon alpha 2b decreases hepatic micrometastasis in a murine model of ocular melanoma by activation of intrinsic hepatic natural killer cells. *Inv Ophthalmol Vis Sci* 45, 2056-2064. 2004.
(27). Bronkhorst IH, jager MJ. Uveal melanoma: the inflammatory microenvironment. *J Innate Immun* 2012;4:454-462.
(28). Lattier JM, Yang H, Crawford S, Grossniklaus HE. Host pigment epithelium-derived factor (PEDF) prevents progression of liver metastasis in a mouse model of uveal melanoma. *Clin Exp Metastasis* 2013;30:969-976.
(29) Ke Q, Costa M. Hypxia-iducible factor-1 (HIF-1). Mol Pharmacol 2006;72:1469-1480.
(30) Notari L, Miller A, Martinez A et al. Pigment epithelium-derived factor is a substrate for matrix metalloproteinase type 2 and type 9: implications for downregulation in hypoxia. *Invest Ophthalmol Vis Sci* 2005;46:2736-2747.
(31) Van den Eynden GG, Majeed AW, Illemann M et al. The multifaceted role of the microenvironment in liver metastasis: biology and clinical implications. *Cancer Res* 2013;73:2031-2043.
(32) Eefsen RL, Van den Eynden GG, Hoyer-Hansen G et al. Histopathological growth pattern, proteolysis and angiogenesis in chemonaive patients resected for multiple colorectal liver metastases. *J Oncol* 2012;2012:907971.
(33) Dithmar SA, Rusciano DA, Armstrong CA, et al. Depletion of NK cell activity results in growth of hepatic micrometastases in a murine ocular melanoma model**.** *Curr Eye Res* 19, 426-431. 1999.
(34) Dayani PN, Gould JE, Brown DB, et al. Hepatic metastasis from uveal melanoma: angiographic pattern predictive of survival after hepatic arterial chemoembolization. *Arch Ophthalmol* 2009;127:628-632
(35) Halenda KM, Kudchadkar RR, Lawson DH, et al. Reduction of nodular growth pattern of metastatic uveal melanoma after radioembolization of hepatic metastases. *Ocul Oncol Pathol* 2016;2:160-165
(36) Xue S, Yang H, Qiao J, et al. Protein MRI contrast agent with unprecedented metal selectivity and sensitivity for liver cancer imaging. *Proc Natl Acad Sci USA*

2015; 112:6607-6612
(37) Yang H, Brackett CM, Morales-Tirado VM et al. The toll-like receptor 5 agonist entolimod suppresses hepatic metastases in a murine model of ocular melanoma via an NK cell-dependent mechanism. *Oncotarget* 2015, epub PMID:26655090

Table 1. Histologic, IHC and IF Findings in Metastastic UM to the Liver

	Infiltrative Pattern				Nodular Pattern			
	single cells	Stage I	Stage II	Stage III	single cells	Stage I	Stage II	Stage III
sinusoidal location	+	+	+	+	-	-	-	-
periportal location	-	-	-	-	+	+	+	+
CD133+ melanoma	+	few	few	-	+	few	few	-
CD56+ NK cells	+	+	few	few	-	-	-	-
CD3+ lymphocytes	-	-	-	-	+	+	few	few
MMP9+ melanoma	-	-	+	-	-	-	+	+
VEGF+ melanoma	-	-	-	-	-	-	+	+
pseudo-sinusoidal spaces	-	-	+	+	-	-	-	-
angiogenesis	-	-	-	-	-	-	-	+

Figure legends.

Figure 1. Number of metastases per area of Stage I, II and III infiltrative and nodular metastases. In the infiltrative pattern, there was a significant decrease in numbers going from StageI to Stage III metastases. In the nodular growth pattern, there was approximately one metastases per 2 cm^2 for all three stages. Standard deviations are shown.

Figure 2. BAP1, CD56 and CD3 expression in melanocytes, NK cells and T lymphocytes. A. There is BAP1 expression (red) in a collection of metastatic UM cells in the liver. B. Collection of metastatic UM cells which are not expressing BAP1. C. There are scattered CD56+ NK cells in the sinusoidal space. D. There are CD3+ cells in the periportal area which includes the bile duct (*) and portal venule (star).
(A and B. BAP1, peroxidase anti-peroxidase with vector red chromagen, 100X. C. CD56, peroxidase anti-peroxidase, 100X. D. CD3, peroxidase anti-peroxidase, 25X)

Figure 3. Single cell infiltrative growth pattern. A. There are metastatic UM cells present in the sinusoidal spaces of the hepatic lobule. B. These single cells include lymphocytes and cells with slightly more eosinophilic cytoplasm. C. The cells with the slightly more cytoplasm express HMB45 (arrows). D. These cell express both HMB45 and CD133 (orange).
(A. H&E 25X, B. H&E 100X, C. HMB45, peroxidase anti-peroxidase with vector red chromagen, 100X, D. Dual labeling for HMB45 green chromagen and CD133 red chromagen, 100X).

Figure 4. Stage 1 infiltrative growth pattern. A. The individual metastatic UM cells in the sinusoidal spaces are clumping and forming small clusters. B. These clusters of melanoma cells, or micrometastases, begin to expand the sinusoidal space. C. The micrometastatic melanoma expresses HMB45. D. Dual labeling for HMB45 (green) and CD 133 (red) show that most of the larger melanoma cells in the micrometastases express only HMB45 whereas small, individual melanoma cells express both HMB45 and CD133 (orange).
(A. H&E 25X, B. H&E 100X, C. HMB45, peroxidase anti-peroxidase with vector red chromagen, 100X, D. Dual labeling for HMB45 (green chromagen) and CD133 (red chromagen), 100X).

Figure 5. Stage 2 infiltrative growth pattern. A. The sinusoidal spaces are filled with metastatic melanoma cells and the hepatocytes have been destroyed. B. The melanoma cells express HMB45. C. Dual labeling for HMB45 (green) and CD133 (red) show that there are many melanoma cells (green) and only rare small individual dual labeled melanoma cells (orange). D. These metastatic UM cells express MMPs (red) and no VEGF (green).
(A. H&E 100X, B. HMB45, peroxidase-anti-peroxidase with vector red chromagen, 100X, C. Dual labeling for HMB45 (green chromagen) and CD133 (red chromagen), 100X D. Dual labeling for HMB45 (green chromagen) and MMP9 (red chromagen), 100X).

Figure 6. Stage 3 infiltrative growth pattern. A. There is complete replacement of the hepatic lobule with islands of melanoma. B. The islands of melanoma express HMB45. C. Dual labeling for HMB45 (green) and CD133 (red) show a only HMB45 expression in the islands of melanoma, although there are rare, small dual labeled cells present. D. There is an absence of VEGF (green) express and MMP (red) expression by the melanoma cells.
(A. H&E 25X, B. HMB45, peroxidase-anti-peroxidase with vector red chromagen, 25X, C. Dual labeling for HMB45 (green chromagen) and CD133 (red chromagen) 100X, D. Dual labeling for VEGF (green chromagen) and MMP (red chromagen), 100X).

Figure 7. Single cell nodular growth pattern. A. Rare individual mononuclear cells (arrow) with slightly more cytoplasm than lymphocytes are identified in fibrous tissue adjacent to the portal venule (*). B. A trichrome stain highlights the collagen within the portal triad which includes the portal venule (*). C. The rare mononuclear cells in this tissue express HMB45. The portal venule is present (*) and there are scattered lymphocytes also present. D. There is dual labeling for HMB45 and CD133 (orange) in rare mononuclear cells in the periportal area (arrows) and within the portal venule (*).
(A. H&E 100X, B. Masson trichrome 100X, C. HMB45 peroxidase anti-peroxidase vector red chromagen 100X, D. Dual labeling for HMB45 green chromagen and CD133 red chromagen, 100X).

Figure 8. Stage 2 nodular growth pattern. A. A well-demarcated nodule of UM cells is present and effaces the surround hepatic lobules. A trichrome stain highlights the portal venule (arrow) within the center of the nodule. B. The melanoma cells in the nodule express HMB45 and surround the portal venule, thus effacing the surround hepatic lobules. C. Melanoma cells express HMB45 (green) and there are no cells that express CD133. D. Dual labeling of the UM cells for VEGF (green) and MMP (red) is seen.
(A. Masson trichrome 10X, B. HMB45 with vector red chromagen, peroxidase anti-peroxidase, 10X, D. HMB45 with green chromagen, CD133 with red chromagen, 10X, F. VEGF with green chromagen, MMP9 with red chromagen, 100X).

Figure 9. Stage 3 nodular growth pattern. A. A nodule of pigmented melanoma cells effaces the adjacent hepatic lobules. A trichrome stain highlights minimal fibrosis surrounding the nodule of melanoma. B. Vascular channels express CD31 in the nodule of melanoma (arrow) and immediately adjacent tissue (*). C. The melanoma expresses HMB45 (green) but not CD133 (red). D. The melanoma co-expresses VEGF (green) and MMP (red), resulting in an orange dual-labeling.
(A. Masson trichrome 10X, B. CD31 peroxidase anti-peroxidase, 10X, C. HMB45 with green chromagen, CD133 with red chromagen, 10X, D. VEGF with green chromagen, MMP with red chromagen, 100X).

Figure 10. Schematic cartoon of metastatic UM to the liver. Melanoma arises in the choroid of the eye (A), extravasates into tumor blood vessels, and then travels via the systemic circulation as circulating melanoma cells with tumor stem cell-like properties (B), where it enters the liver as single cells. These single cells likely arise from hepatic

arterioles and seed the sinusoidal space causing the *infiltrative pattern* of growth, which progresses to Stage 1 (0-50μm) micrometastases, Stage 2 intermediate (51-500μm) metastases which are bathed by serum in the sinusoidal space, and eventually Stage 3 (>501μm) metastases which replace the hepatic lobule, do not express MMP9/VEGF or display angiogenesis. Alternatively, circulating melanoma cells may enter the liver via the portal venule causing the nodular growth pattern, first as single cells, then Stage 1 (0-50μm) micrometastases that co-opt the portal venule, then Stage 2 (51-500μm) intermediate metastases that begin to efface the adjacent hepatic lobule, and finally Stage 3 (>501μm) metastases which express MMP9/VEGF, display angiogenesis and further efface the adjacent hepatic lobule.

Figure 11. Schematic cartoon of proposed mechanisms of infiltrative and nodular growth patterns of metastatic UM to the liver. UM cells with tumor stem cell-like properties extravasate from the primary ocular tumor and disseminate hematogenously to the liver. In the *infiltrative* growth pattern, these UM cells may metastasize to the sinusoidal spaces in the parenchyma of the hepatic lobule and grow from single melanoma cells to Stages I-III metastases. This infiltrative growth is related in part to a change in the immune microenvironment within the sinusoidal space, including downregulation of NK cells.[26,32] Hypoxia results in MMP production in Stage II which allows for tissue dissection and creation of pseudosinusoidal spaces. Micrometastases receive their nutrition form blood in the sinusoidal space; larger metastases are bathed by blood in pseudosinusoidal spaces.[8] In the *nodular* growth pattern, circulating UM cells metastasize to the periportal areas in the hepatic triad, co-opt the portal venules for nutrition, and progress from single UM cells to Stages I-III metastases. Hypoxia results in MMP production and VEGF expression. Nodular growth is related in part to MMP degradation of PEDF, increased VEGF expression by melanoma cells, an increased VEGF:PEDF ratio and angiogenesis.

Figures

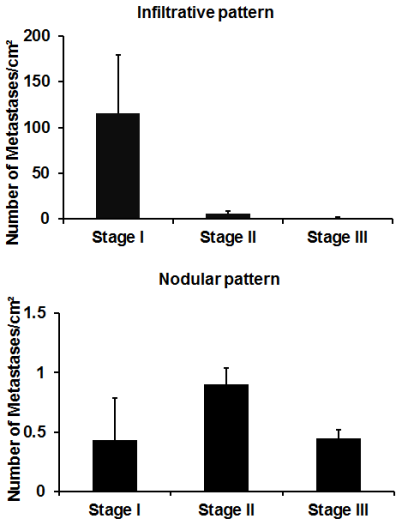

Fig 1

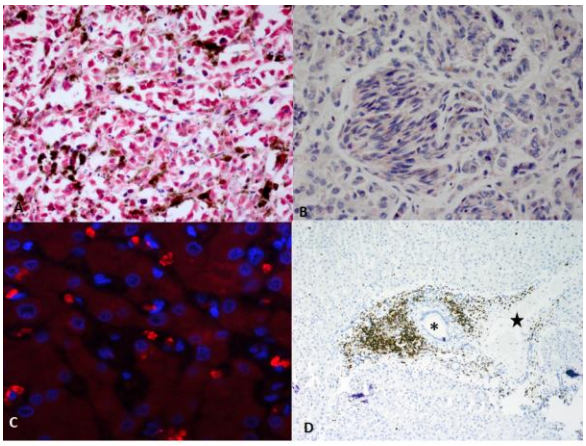

Fig 2

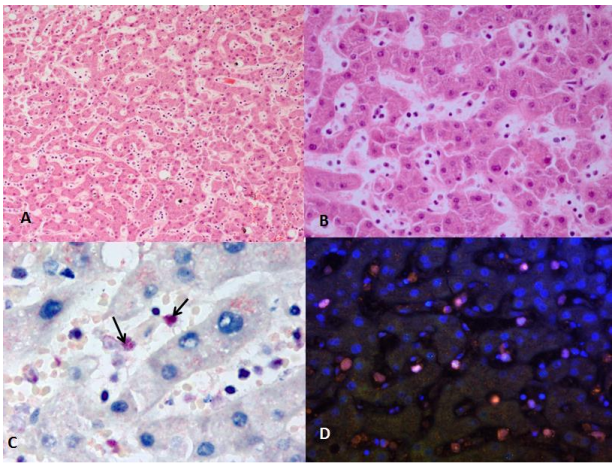

Fig 3

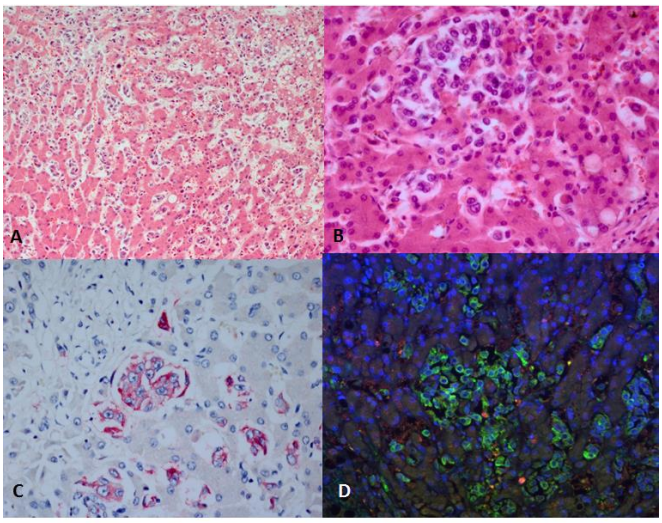

Fig 4

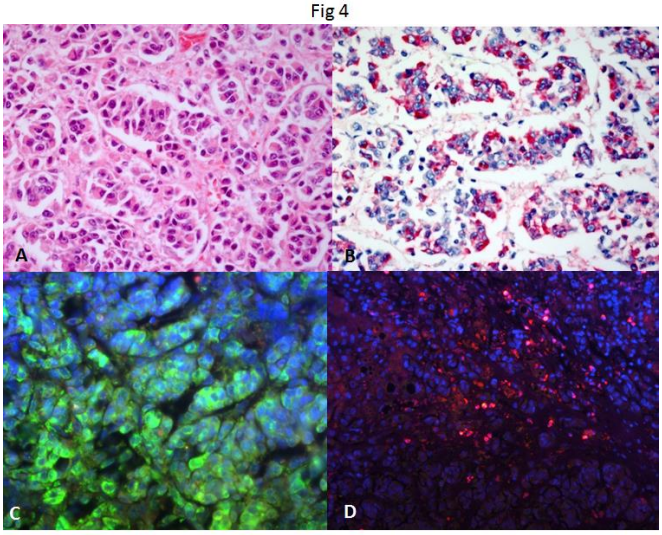

Fig 5

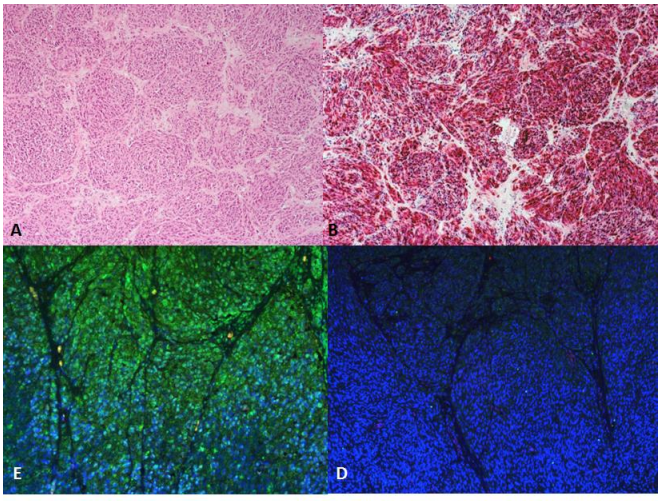

Fig 6

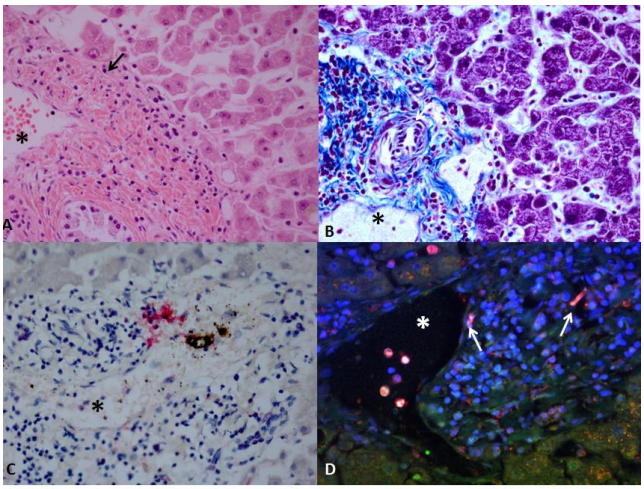

Fig 7

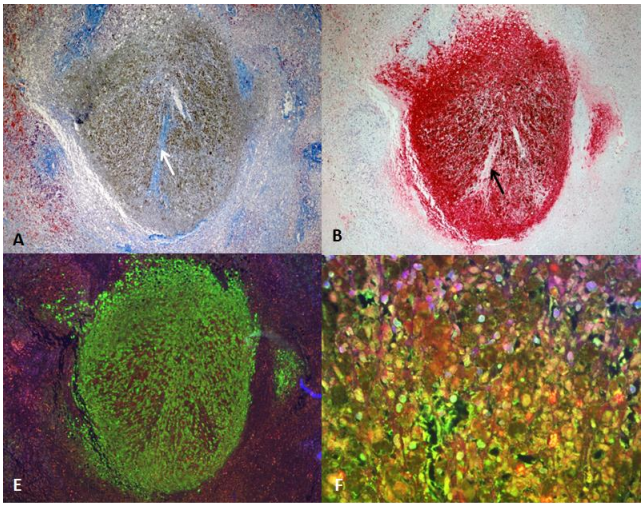

Fig 8

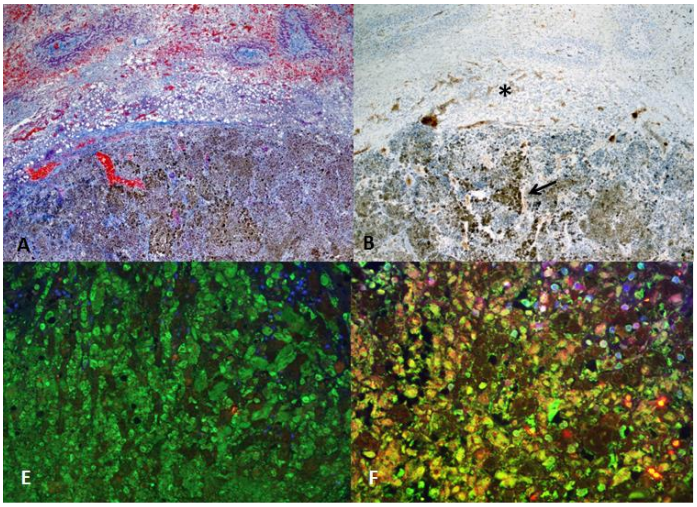

Fig 9

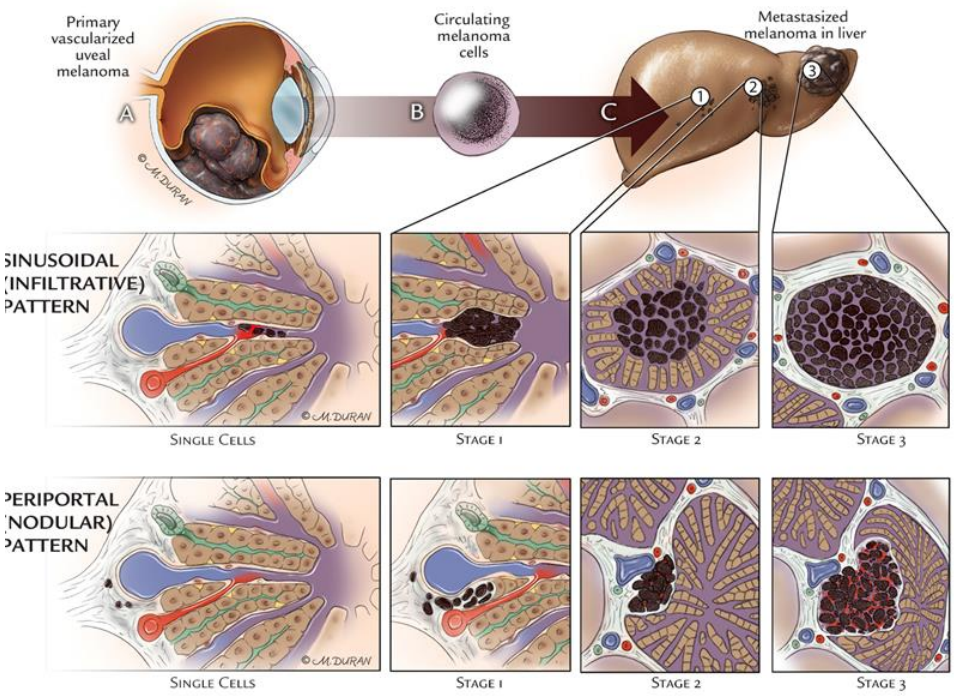
Primary vascularized uveal melanoma
Circulating melanoma cells
Metastasized melanoma in liver
A
B
C
1
2
3
SINUSOIDAL (INFILTRATIVE) PATTERN
PERIPORTAL (NODULAR) PATTERN
SINGLE CELLS
STAGE 1
STAGE 2
STAGE 3

Fig 10

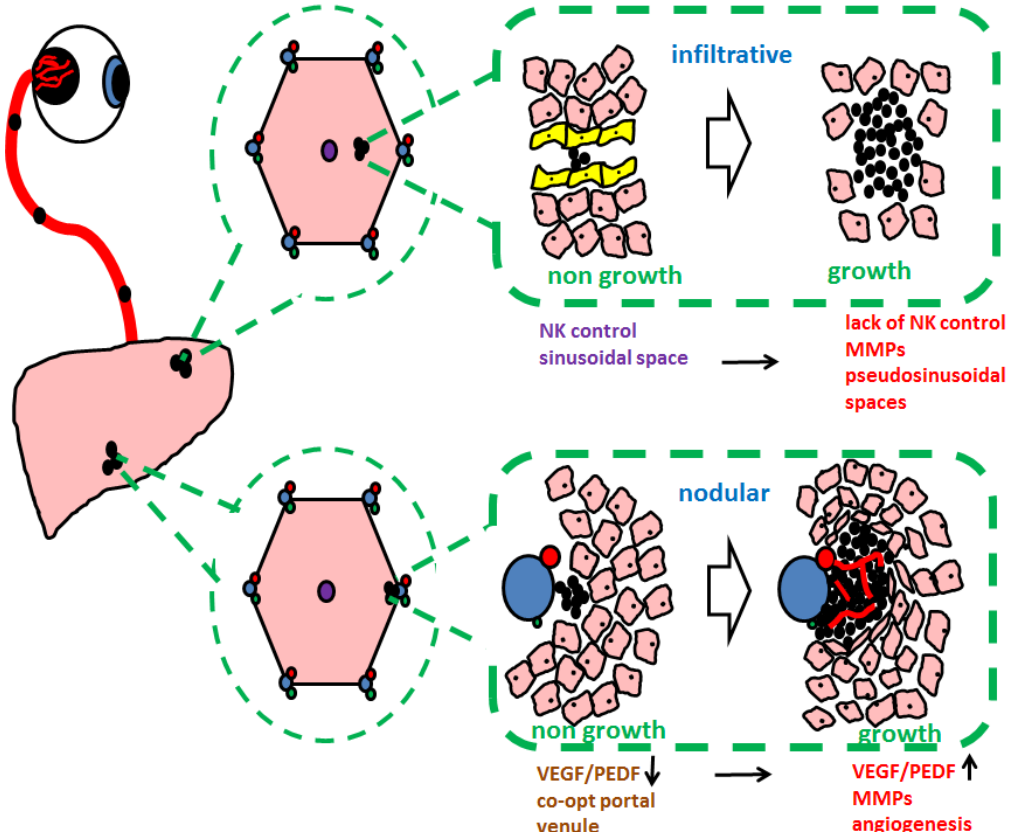
infiltrative
non growth
growth
NK control
sinusoidal space
lack of NK control
MMPs
pseudosinusoidal
spaces
nodular
non growth
growth
VEGF/PEDF
co-opt portal
venule
VEGF/PEDF
MMPs
angiogenesis

Fig 11